Volume 15
Number 31
21 August 2024
Pages 12151–12618

Chemical Science

rsc.li/chemical-science

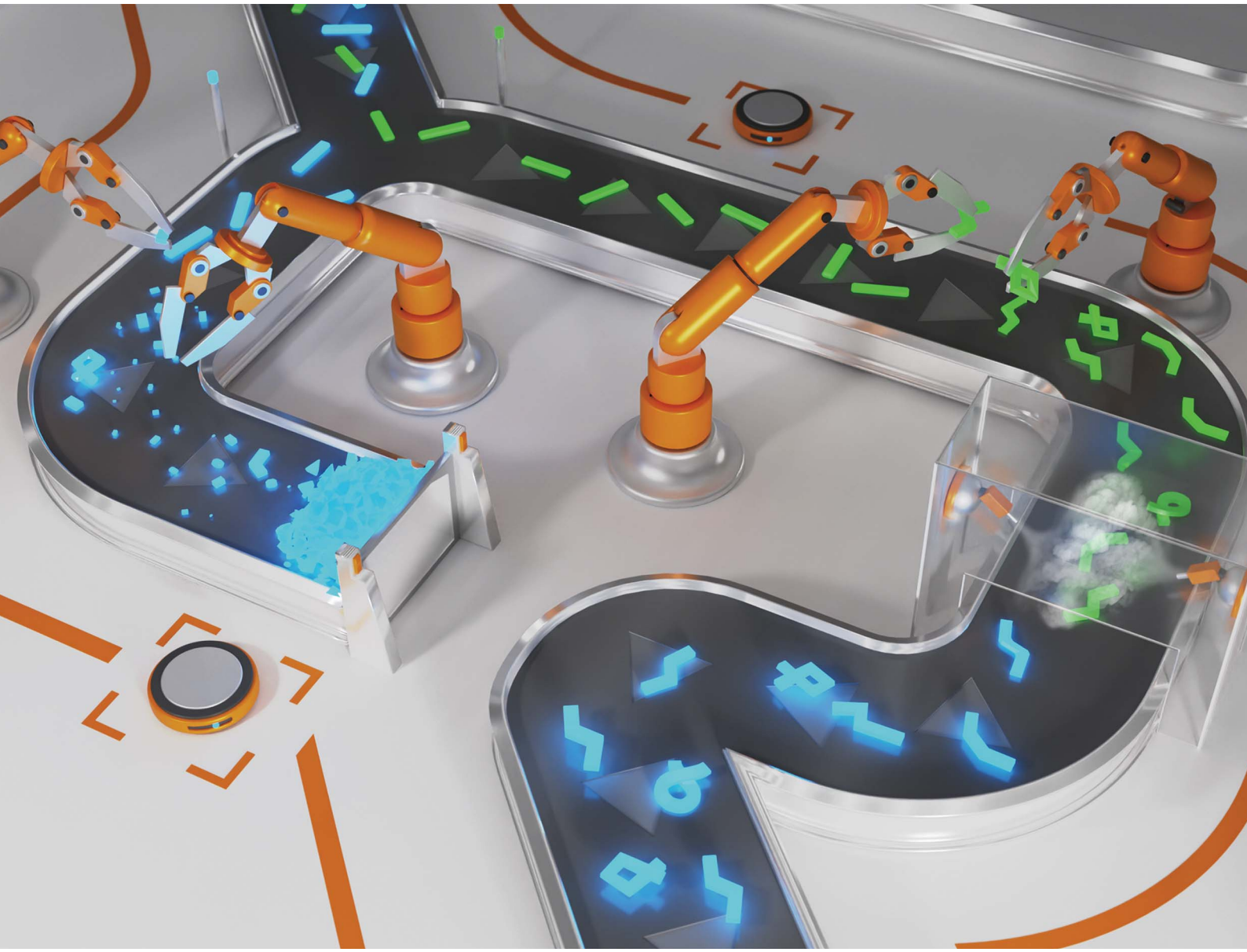

ISSN 2041-6539

ROYAL SOCIETY OF CHEMISTRY

EDGE ARTICLE
Tomohiro Seki *et al.*
Preparation of intrinsically fragile bent crystals

Chemical Science

ROYAL SOCIETY OF CHEMISTRY

EDGE ARTICLE

View Article Online
View Journal | View Issue

Cite this: *Chem. Sci.*, 2024, **15**, 12258

All publication charges for this article have been paid for by the Royal Society of Chemistry

Received 3rd May 2024
Accepted 6th July 2024

DOI: 10.1039/d4sc02918f

rsc.li/chemical-science

Preparation of intrinsically fragile bent crystals†

Tomohiro Seki, *[a] Shiori Kobayashi,[a] Rintaro Ishikawa,[a] Keigo Yano,[b] Takumi Matsuo [bc] and Shotaro Hayashi [bc]

Although molecular crystals have long been considered to be intrinsically brittle, a study of molecular crystals that are capable of plastic or elastic bending upon applying mechanical stress recently attracted significant attention. Malleable molecular crystals often need to meet specific criteria regarding the intermolecular interaction patterns within the crystal structure. Accordingly, examples have been reported where one polymorph shows bending, while other polymorphs of the same compound exhibit fracturing upon exposure to mechanical force. Here, we have succeeded in preparing bent crystals of an intrinsically fragile polymorph. Methylated flufenamic acid (**1**) can form three different polymorphs, *i.e.*, **1α**, **1β**, and **1γ**, of which **1β** is difficult to isolate. Under mechanical force, the crystals of **1α** exhibit remarkable plastic deformation, while those of **1γ** are readily broken. Similar to the mechanical properties, the emission properties of **1** differ depending on the polymorph, *i.e.*, **1γ** exhibits a shorter-wavelength emission maximum and much higher emission quantum yield than **1α**. Remarkably, both the unbent and bent forms of the **1α** crystals can undergo a phase transition to the **1γ** phase upon exposure to ethyl acetate. In this manner, phase transitions of the mechanically bent crystals of polymorph **1α** afforded bent crystals of the intrinsically fragile polymorph **1γ**. These findings may lead to a potential post-modification method for the preparation of functional flexible materials with enhanced emission properties in order to expand their applications.

Introduction

Molecular crystals have long been considered to be intrinsically brittle. Although they often show unique optoelectronic properties that stem from their anisotropy and dense packing, their brittle nature has hampered their applications in the development of advanced materials.[1] However, the past few decades have witnessed numerous reports of molecular crystals that are capable of plastic or elastic bending upon applying mechanical stress. In particular, functional bendable crystals have provided new applications in flexible optoelectronic materials,[2] such as optical waveguides,[3] conductivity,[4] ferro/piezoelectricity,[5] and hybridization with a polymer.[6]

Several studies have found that intermolecular interaction patterns within molecular crystals are important for their bending behavior.[7] For example, bendable molecular crystals often adopt molecular arrangements that exhibit anisotropy in terms of the strength of the intermolecular interactions. Typically, molecules in plastically bendable crystals exhibit stacking arrangements to form tightly packed column motifs. The columns exhibit strong intermolecular interactions with neighboring columns along one of the two directions orthogonal to the column axis, and weak interactions along the other orthogonal direction.[7a,b,e] When the intermolecular interactions manifest along the two orthogonal directions with respect to the column axis are energetically comparable, elastic bending behavior is often observed.[7c,f,g] These results indicate that control over the molecular arrangement is required to achieve bending in molecular crystals.

Polymorphism-dependent crystal-bending behavior has also been reported. Generally, different polymorphs exhibit different properties, such as emission or semiconducting properties, despite the constituent molecule being the same.[8] Similarly, the mechanical properties of molecular crystals can differ among their polymorphs.[9] Desiraju *et al.* reported that three polymorphs of 4-bromophenyl-4-bromobenzoate show plastic deformation, elastic deformation, and fracture under mechanical stress.[9a] In addition, the mechanical properties of crystals can be controlled through phase transitions between polymorphs. For example, Zhang reported a thermal phase transition from polymorph A to polymorph B of 9,10-bis(phenylethynyl)anthracene; these polymorphs exhibit plastic bending and fracture, respectively, when subjected to mechanical force under ambient conditions.[9c] However, reports

[a]*Department of Chemistry, Faculty of Science, Shizuoka University, Shizuoka City, Shizuoka 422-8017, Japan. E-mail: seki.tomohiro@shizuoka.ac.jp*

[b]*School of Engineering Science, Kochi University of Technology, 185 Miyanokuchi, Tosayamada, Kami, Kochi 782-8502, Japan*

[c]*Research Institute, Kochi University of Technology, 185 Miyanokuchi, Tosayamada, Kami, Kochi 782-8502, Japan*

† Electronic supplementary information (ESI) available: X-ray crystallographic data, optical microscopy images, thermal data, emission spectra and other additional information. CCDC 2350732–2350734. For ESI and crystallographic data in CIF or other electronic format see DOI: https://doi.org/10.1039/d4sc02918f

of phase transitions in bent crystals remain limited so far.[10] Such phase transitions should enable "post-modification" of the properties or the shape of mechanically processed bent crystals.

Here, we report methylated flufenamic acid **1**,[11] which can be used to prepare an intrinsically fragile bent crystal based on its polymorph-dependent mechanical and phase-transition properties (Fig. 1). **1** forms three different polymorphs, *i.e.*, **1α**, **1β**, and **1γ**, although **1β** is difficult to isolate in synthetically meaningful amounts. **1α** is plastically deformed under mechanical stress, while **1γ** is fractured. Crystal-structure analyses confirmed that the packing arrangement of **1α** exhibits characteristics typical of plastically bendable molecular crystals. In contrast, **1γ** does not exhibit this type of crystal structure. Vapor treatment resulted in an interpolymorph phase transition from **1α** to **1γ**. Remarkably, the bent crystals of **1α** also undergo phase transitions by vapor treatment to give bent crystals of the intrinsically brittle polymorph **1γ**.

Results and discussion

Compound **1**[11e] forms three different polymorphs, *i.e.*, **1α**, **1β**, and **1γ**, under different crystallization conditions. Weakly green-emitting polymorph **1α** was obtained by slow evaporation of **1** in methanol for three days. Using the same solution, evaporation over seven days afforded polymorph **1β**. However, the concomitant formation of **1α** and **1β** made the isolation of **1β** in synthetically meaningful amounts difficult, which limited our ability to perform several of the experiments for **1β**. **1γ** was obtained from an ethanol/H_2O (4 : 1) solution of **1** and NH_4Cl, as reported by Byrn for the crystallization of form V of flufenamic acid.[11a] A mixture of **1** and NH_4Cl in ethanol/H_2O was filtered and left to stand for three days under ambient conditions to give crystals of **1γ**.

Upon applying mechanical stress, the crystals of **1α** and **1β** bend plastically, while the crystal of **1γ** breaks. Applying

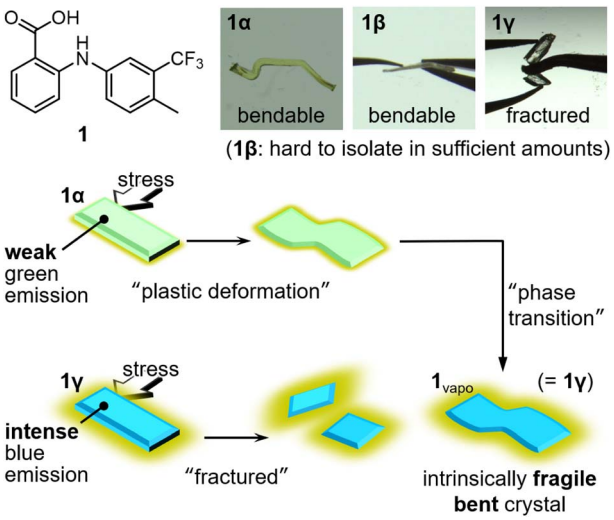

Fig. 1 Chemical structure of **1**. Photographs of **1α**, **1β**, and **1γ**. Schematic representation of polymorphism and mechanical properties of the crystals of **1**.

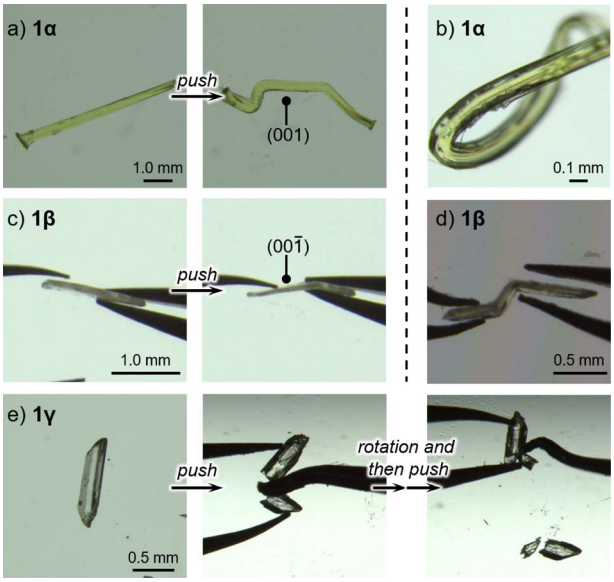

Fig. 2 Photographs of pieces of crystals of (a) **1α**, (c) **1β**, and (e) **1γ** before and after applying mechanical stress. Photographs of the most extremely bent crystals of (b) **1α** and (d) **1β**.

mechanical stress to the (001) plane of **1α** resulted in a dramatic change in its shape (Fig. 2a and S1 as well as ESI Movie S1†). After removing the stress, **1α** retains its deformed shape, confirming the occurrence of plastic deformation. When mechanical stress was applied to the other faces of the crystal of **1α**, the crystals fractured (Fig. S2†). The crystals of **1β** also displayed plastic deformation upon applying mechanical stress to the (00−1) face (main face, Fig. 2c), but broke when the other crystal faces (minor faces) were pushed (Fig. S3†). Repeated tests revealed that the bending behavior of **1α** is much more dramatic than that of **1β** (Fig. 2b and d, respectively). Unlike the crystals of **1α** and **1β**, those of **1γ** were found to be mechanically brittle. Irrespective of the face to which the stress was applied, the crystals of **1γ** fractured under mechanical stress (Fig. 2e).[12] These differences in the mechanical properties of **1** should originate from their different crystal structures.

A single-crystal X-ray diffraction (XRD) analysis of **1α** indicated the presence of slide planes responsible for plastic bending. **1α** crystalized in the $Pna2_1$ space group (Fig. 3 and S5 as well as Table S1†). The dihedral angles of the two benzene rings of each molecule (θ_d) were determined to be 136.77° and 138.82° ($Z' = 2$). As typically observed for molecular crystals that contain benzoic-acid groups,[13] double hydrogen bonding interactions were observed (O···O distance: 2.640 Å; Fig. 3a). The resulting flat planes formed by two benzoic-acid moieties within the dimer stack with the neighboring flat planes of other dimers with an offset result in the formation of a column structure (Fig. 3b, c and S5†). These columns interact tightly with each other along the *a* axis through CH–π interactions (3.845 or 3.869 Å for the carbon–π plane distance; dashed lines in Fig. 3d) to form sheet-like architectures along the (001) plane. In contrast, no clear "strong" intermolecular interactions are present between the columns along the *c* direction, where the

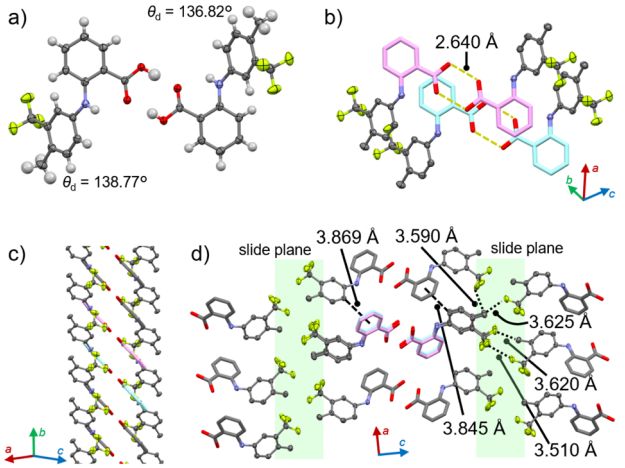

Fig. 3 Crystal structure of **1α** showing (a) the dimer, (b) the stacked dimers, (c) the column, and (d) the interactions among the columns.

CF_3 and Me groups are oriented (highlighted in green, Fig. 3d). These moieties should act as slide planes along which the molecules within the sheet motif move upon the plastic bending of the crystal.[14] Such molecular movements along slide planes have been reported for plastically bending crystals.[7a,b,e] An energy-framework analysis based on the crystal structure of **1α** corroborated a pronounced anisotropy of the strength of the intermolecular interactions (Fig. S6†).[15]

1γ also forms a column motif through the stacking of doubly hydrogen-bonded dimers, but unlike **1α**, it does not feature slide planes. Polymorph **1γ** crystallizes in the $P2_1/n$ space group (Fig. 4 and S8 as well as Table S1†). Similar to **1α**, the conformation of **1** is twisted (θ_d = 45.91°; Fig. 4a). The difference between the θ_d of **1α** and **1γ** is ~90°, indicating that the orientation of the CF_3 groups is the main difference between the monomer conformations in the two polymorphs (Fig. S9†). The hydrogen-bonded dimers in **1γ** (O···O distance: 2.649 Å; Fig. 4a) stack to form a column along the *a* axis through the parallel orientation of the planes formed by the benzoic-acid domains (Fig. 4b, c and S8†). These columns interact along both the *b* and *c* directions *via* weak CH···F interactions (dotted lines in Fig. 4d). This is different from the intercolumnar interactions in **1α**, in which the columns form sheets through relatively strong CH–π interactions. The energy-framework analysis of **1γ** also showed a less pronounced anisotropy of the strength of the intermolecular interactions along the *b* and *c* axes (Fig. S10†) compared to that of **1α**. Thus, **1γ** does not have slide planes, which are often observed in the crystal structures of plastically bendable molecular crystals such as **1α**.[7a,b,e] This is in agreement with the absence of plastic deformation of **1γ** upon applying mechanical stress (Fig. 2e).

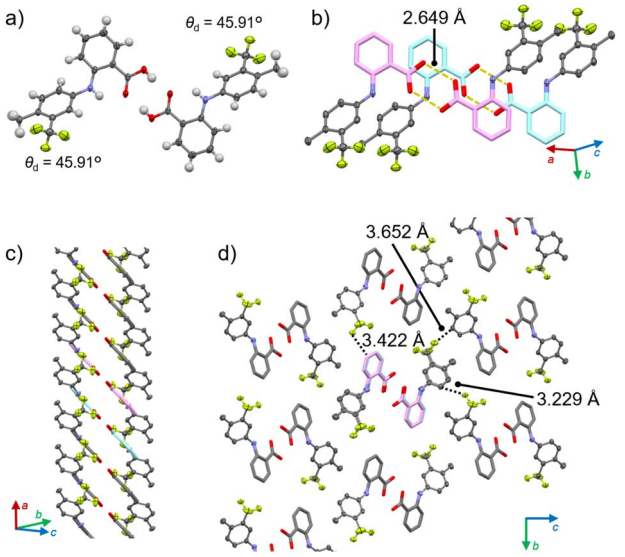

Fig. 4 Crystal structure of **1γ** showing (a) the dimer, (b) the stacked dimers, (c) the column, and (d) the interactions among the columns.

An investigation into the photophysical properties of **1** revealed that mechanically brittle **1γ** exhibits a much higher absolute emission quantum yield (Φ_{em}) than **1α**. Under photoexcitation at 365 nm, the crystal of green-emitting **1α** showed broad emission with a maximum wavelength ($\lambda_{em,max}$) of 469 nm and an Φ_{em} of 5.6% (Fig. 5 and Table S2†). The emission–decay profile of **1α** provides an average emission lifetime (τ_{av}) of 0.66 ns (Fig. S11 and Table S2†), which indicates that the emission of **1α** can be assigned to fluorescence, similar to the case of flufenamic acid.[11c,d] In contrast, blue-emitting **1γ** displays a broad emission spectrum ($\lambda_{em,max}$ = 437 nm) that is hypsochromically shifted relative to that of **1α** (Fig. 5). The τ_{av} of **1γ** was determined to be 3.9 ns (Fig. S11 and Table S2†), indicating that the emission of **1γ** should also be attributed to fluorescence. The absorption spectral onset wavelength of **1γ** is also located in a shorter wavelength region (~430 nm) than that of **1α** (~470 nm; Fig. S12†).[16] Remarkably, the Φ_{em} value of **1γ** was determined to be 51%, which is roughly nine times that of **1α** (Fig. 5 and Table S2†). The low Φ_{em} of **1α** could be due to the presence of the slide planes, given that the crystal-structure domains with weak intermolecular interactions in the slide planes could promote the nonradiative quenching pathway. These results indicate that the photophysical properties of **1** depend on the polymorph, similar to their mechanical properties, which suggests that if phase transitions between the polymorphs of **1** could be achieved, these properties could be controlled.

Vapor treatment of **1α** resulted in a phase transition to **1γ**, accompanied by changes in the mechanical and emission

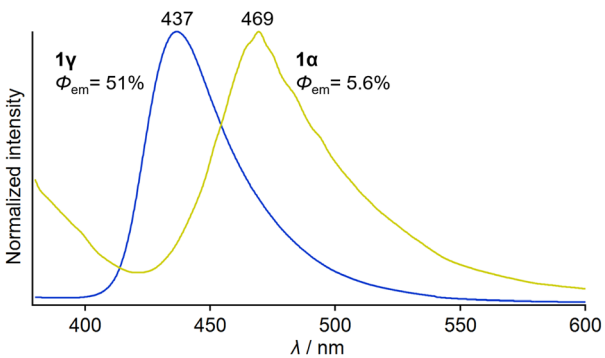

Fig. 5 Emission spectra of **1α** and **1γ** under excitation at 365 nm.

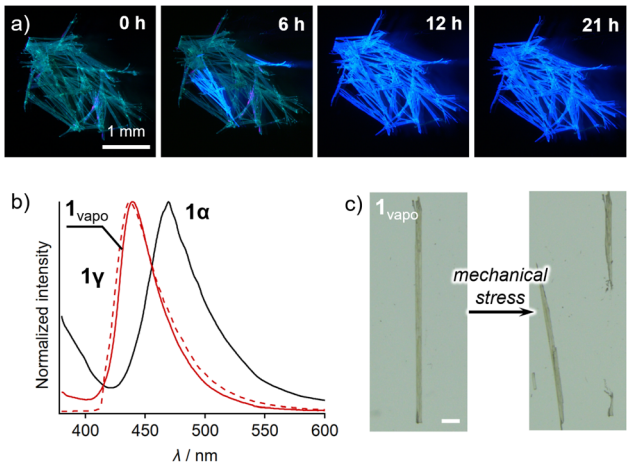

Fig. 6 (a) Photographs of the transformation of **1α** into $\mathbf{1}_{vapo}$ upon exposure to ethyl acetate recorded under irradiation with UV light. (b) Emission spectra of **1α**, **1γ**, and $\mathbf{1}_{vapo}$ under excitation at 365 nm. (c) Photographs of a piece of a $\mathbf{1}_{vapo}$ crystal before and after the application of mechanical stress; white scale bars in (c) represent 0.5 mm.

properties. After exposure to ethyl acetate for 24 h, the solid sample of **1α** changed color from yellow to white (Fig. S15†). Simultaneously, the emission color changed from blue-green to blue with intensified emission intensity (Fig. 6a). The resulting samples are hereafter called $\mathbf{1}_{vapo}$.[17] Interestingly, the absorption and emission spectra and the emission–decay profiles of $\mathbf{1}_{vapo}$ were different from those of **1α** and resemble those of **1γ** (Fig. S12, 6b and S11,† respectively). Moreover, single-crystal XRD analysis of the $\mathbf{1}_{vapo}$ crystal revealed that the crystallographic parameters of $\mathbf{1}_{vapo}$ were essentially identical to those of **1γ** obtained from recrystallization (Table S3†). Similarly, the DSC traces of $\mathbf{1}_{vapo}$ resemble those of **1γ** (Fig. S17†). These results indicate that the phase transition of **1α** to a phase similar to that of **1γ** occurs upon exposure to ethyl-acetate vapor. Other good solvents, such as acetone and chloroform, can also promote the phase transition from **1α** to **1γ** (Fig. S18†). As a result of the phase transition from **1α** to $\mathbf{1}_{vapo}$ (=**1γ**), the emission color changed (Fig. 6b), accompanied by a marked increase in emission intensity (Φ_{em}: 5.6 → 46%; Fig. S19 and Table S2†). Similarly, the mechanical properties of **1** were modulated, *i.e.*, the bendable **1α** became brittle upon vapor treatment when $\mathbf{1}_{vapo}$ is formed (Fig. 6c). The thermal phase transition from **1α** to **1γ** phases also occurred, as confirmed by spectroscopic and powder XRD analyses (Fig. S20†).[18] These results indicate that the vapor treatment of **1** induces a phase transition from **1α** to the thermodynamically favorable phase **1γ**.

By utilizing the phase transition behavior of **1**, bent crystals of intrinsically brittle **1γ** can be obtained. A pristine crystal of **1α** was bent *via* mechanical force and then exposed to ethyl-acetate vapor (Fig. 7). This bent crystal of **1α** also underwent an emission color change (Fig. 7). The resulting emission spectrum essentially overlaps with that of **1γ** (Fig. S21†), similar to the spectrum of the unprocessed crystal of **1α** (Fig. 6b). This result indicates that the bent crystal **1α** underwent the phase

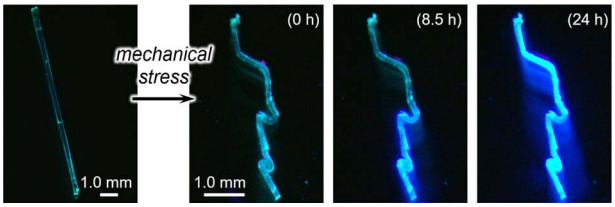

Fig. 7 Photographs of unbent and bent **1α** and bent $\mathbf{1}_{vapo}$ recorded under irradiation with UV light. The exposure time to ethyl-acetate vapor is shown in parentheses.

transition to $\mathbf{1}_{vapo}$ (=**1γ**). The transition was also supported by a single-crystal XRD study of a small piece of a bent $\mathbf{1}_{vapo}$ crystal, which was cut off from a larger crystal (Table S3†). The resulting bent $\mathbf{1}_{vapo}$ crystal showed intense green emission (Fig. 7). Importantly, **1γ** is intrinsically brittle under mechanical force (Fig. 2e). Thus, the "intrinsically brittle" bent crystal $\mathbf{1}_{vapo}$ (=**1γ**) can only be obtained through a vapor-induced phase transition from the bent crystal of malleable **1α**. This method will possibly lead to new applications that require both a bent crystal shape and novel emission properties.

The slow phase transition from **1α** to **1γ** could be the key to retaining the bent shape of the crystals. In previously reported studies that investigated the phase transitions of the mechanically bent crystals, the phase transitions induce the crystal-shape changes to recover the original straight shape or to further bend the shape.[10a–d] Importantly, these phase transitions occur in a time frame of minutes or less.[10a–d] Such rapid phase changes often result in accumulated internal strain within the crystalline lattice, especially at interfaces between the parent and the converted domains.[10a] The crystal-shape changes then occur as a result of releasing this strain. On the other hand, the vapor-induced phase transition of **1** takes 20 h or more, most likely due to the relatively large conformational change including the ~90° rotation of the CF_3-substituted benzene ring of **1** (Fig. S9†). Such slow crystal-structure changes prevent the accumulation of residual strain within the interface. Thus, molecular-arrangement changes in **1** do not lead to a change in the shape of the crystal morphology.

The pristine polymorphs **1α** and **1γ** were both found to exhibit optical waveguide behavior. Molecular crystals with optical waveguide properties have potential for various applications in optoelectronics and flexible materials.[3,19] To assess the waveguide properties of **1**, their pristine crystals were photoexcited *via* irradiation with focused laser light (λ_{ex} = 405 nm) at specific positions, and the emission spectra were monitored at the edge positions (Fig. 8a, b and S22†). The ratio of the emission intensity at the excitation point (I_{Ex}) and crystal edge (I_{WG}) was plotted as a function of the distance (D) between the excitation and detection points (Fig. 8 and S23†). Both polymorphs **1α** and **1γ** exhibited decreasing I_{WG}/I_{Ex} values with increasing D (Fig. 8c and d, respectively), indicating their waveguide activity. Furthermore, the plots were fitted using the relationship $I_{WG}/I_{Ex} = A\exp(-\alpha D)$, where A is a constant and α is the loss coefficient.[19c] The results suggest α values of 0.013 ± 0.005 dB μm^{-1} and 0.044 ± 0.003 dB μm^{-1} for **1α** and **1γ**,

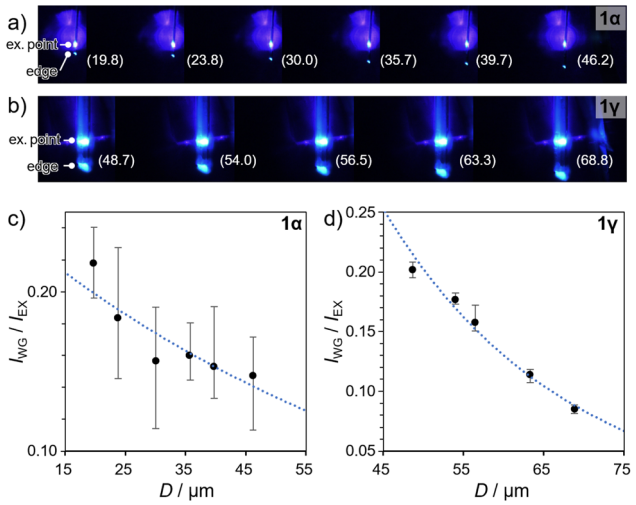

Fig. 8 (a) Fluorescence images of (a) pristine **1α** and (b) pristine **1γ** with laser excitation (λ_{ex} = 405 nm) applied at different positions along the long-axis direction. The distance between the excitation and detection points (D in μm) is denoted in parentheses. Magnified images are shown in Fig. S22.† (c) Ratios of the emission intensity I_{WG}/I_{Ex} plotted as a function of D for (c) **1α** and (d) **1γ**, corresponding to the images in (a) and (b), respectively.

respectively. The smaller α value of **1α** indicates its superior waveguide behavior compared to that of **1γ**. Unfortunately, subjecting **1α** to bending or phase transitions led to a loss of its waveguide properties, *i.e.*, the bent crystals of **1α** and the crystal of $\mathbf{1}_{vapo}$ did not show waveguide properties (data not shown). This result indicates that the current process of changing the shape or molecular arrangement of the crystals causes a deterioration of the molecular order, which severely affects their specific optical properties, *i.e.*, their waveguide activity. Ideally, the application of external stimulation in an optimized manner, *i.e.*, gentle pushing to bend **1α** or pressure/concentration control during vapor exposure for the transformation of **1α** into $\mathbf{1}_{vapo}$, could prevent the deterioration of the molecular arrangement within the resulting crystals, allowing the waveguide activity to be retained. The achievement of waveguide activity in bent $\mathbf{1}_{vapo}$ is our future goal.

Conclusions

In conclusion, we have reported the mechanical and emission properties, as well as the phase-transition behavior of two predominant polymorphs of **1**, *i.e.*, **1α** and **1γ**. The crystals of **1α** with a low Φ_{em} of 5.6% exhibit dramatic plastic bending upon exposure to mechanical stress. In contrast, the crystals of **1γ**, which exhibit pronounced emission properties (Φ_{em} = 51%), are brittle and break upon exposure to mechanical stress. Treatment of crystals of **1α** with ethyl-acetate vapor induces a phase transition, even after these crystals had undergone mechanical deformation, thus allowing the preparation of bent-shaped **1γ** crystals ($\mathbf{1}_{vapo}$). This indicates that through exploitation of the polymorph-dependent emission and mechanical properties in conjunction with the phase-transition capability, we successfully achieved the preparation of a novel optically active bent crystal of an intrinsically fragile polymorph. This method can be used as a post-modification technique for the preparation of functional flexible materials to enhance the emission properties in order to expand their application portfolio.

Data availability

The data supporting this article have been included as part of the ESI.† Crystallographic data for **1α**, **1β**, and **1γ** has been deposited at the CCDC with CCDC# of 2350732, 2350733, and 2350734, respectively, and can be obtained from **https://www.ccdc.cam.ac.uk/**.

Author contributions

T. S. designed the project; all experiments except for the waveguide experiments were performed and analyzed mostly by S. K. and partially by R. I. with guidance from T. S.; K. Y. and S. H. performed and analyzed the nanoindentation experiments; T. M. and S. H. performed and analyzed the waveguide experiments; T. S. wrote the manuscript.

Conflicts of interest

There are no conflicts to declare.

Acknowledgements

This work was financially supported by JSPS KAKENHI grants JP22H021550, JP22K190580, and JP24K01574 as well as by JST PRESTO (JPMJPR21AB) and JST FOREST Program (JPMJFR211W) (Japan).

Notes and references

1 (*a*) S. Hayashi, *Polym. J.*, 2019, **51**, 813–823; (*b*) S. K. Park and Y. Diao, *Chem. Soc. Rev.*, 2020, **49**, 8287–8314; (*c*) W. M. Awad, D. W. Davies, D. Kitagawa, J. M. Halabi, M. B. Al-Handawi, I. Tahir, F. Tong, G. Campillo-Alvarado, A. G. Shtukenberg, T. Alkhidir, Y. Hagiwara, M. Almehairbi, L. Lan, S. Hasebe, D. P. Karothu, S. Mohamed, H. Koshima, S. Kobatake, Y. Diao, R. Chandrasekar, H. Zhang, C. C. Sun, C. Bardeen, R. O. Al-Kaysi, B. Kahr and P. Naumov, *Chem. Soc. Rev.*, 2023, **52**, 3098–3169; (*d*) M. Hasegawa and K. Ishii, *Chem.–Eur. J.*, 2019, **25**, 5105.

2 (*a*) A. J. Thompson, A. I. Chamorro Orué, A. J. Nair, J. R. Price, J. McMurtrie and J. K. Clegg, *Chem. Soc. Rev.*, 2021, **50**, 11725–11740; (*b*) S. Ghosh and M. K. Mishra, *Cryst. Growth Des.*, 2021, **21**, 2566–2580; (*c*) T. Seki, N. Hoshino, Y. Suzuki and S. Hayashi, *CrystEngComm*, 2021, **23**, 5686–5696; (*d*) C. Wei, L. Li, Y. Zheng, L. Wang, J. Ma, M. Xu, J. Lin, L. Xie, P. Naumov, X. Ding, Q. Feng and W. Huang, *Chem. Soc. Rev.*, 2024, **53**, 3687–3713.

3 W. Wu, K. Chen, T. Wang, N. Wang, X. Huang, L. Zhou, Z. Wang and H. Hao, *J. Mater. Chem. C*, 2023, **11**, 2026–2052.

4 Y. Chen, Z. Chang, J. Zhang and J. Gong, *Angew. Chem., Int. Ed.*, 2021, **60**, 22424–22431.
5 M. Owczarek, K. A. Hujsak, D. P. Ferris, A. Prokofjevs, I. Majerz, P. Szklarz, H. Zhang, A. A. Sarjeant, C. L. Stern, R. Jakubas, S. Hong, V. P. Dravid and J. F. Stoddart, *Nat. Commun.*, 2016, **7**, 13108.
6 For the hybridization of elastic crystals and polymeric materials in order to endow bendable molecular crystals with vapor responsivity, see: L. Lan, X. Yang, B. Tang, X. Yu, X. Liu, L. Li, P. Naumov and H. Zhang, *Angew. Chem., Int. Ed.*, 2022, **61**, e202200196.
7 (*a*) C. M. Reddy, M. T. Kirchner, R. C. Gundakaram, K. A. Padmanabhan and G. R. Desiraju, *Chem.–Eur. J.*, 2006, **12**, 2222–2234; (*b*) C. M. Reddy, K. A. Padmanabhan and G. R. Desiraju, *Cryst. Growth Des.*, 2006, **6**, 2720–2731; (*c*) S. Ghosh, M. K. Mishra, S. B. Kadambi, U. Ramamurty and G. R. Desiraju, *Angew. Chem., Int. Ed.*, 2015, **54**, 2674–2678; (*d*) T. Seki and H. Ito, *Chem.–Eur. J.*, 2016, **22**, 4322–4329; (*e*) M. K. Panda, K. B. Pal, G. Raj, R. Jana, T. Moriwaki, G. D. Mukherjee, B. Mukhopadhyay and P. Naumov, *Cryst. Growth Des.*, 2017, **17**, 1759–1765; (*f*) S. Hayashi, T. Koizumi and N. Kamiya, *Cryst. Growth Des.*, 2017, **17**, 6158–6162; (*g*) M. Đaković, M. Borovina, M. Pisačić, C. B. Aakeröy, Ž. Soldin, B. M. Kukovec and I. Kodrin, *Angew. Chem., Int. Ed.*, 2018, **57**, 14801–14805.
8 (*a*) L. Yu, *Acc. Chem. Res.*, 2010, **43**, 1257–1266; (*b*) J. Bernstein, *Cryst. Growth Des.*, 2011, **11**, 632–650.
9 (*a*) S. Saha and G. R. Desiraju, *Chem. Commun.*, 2018, **54**, 6348–6351; (*b*) B. Tang, B. Liu, H. Liu and H. Zhang, *Adv. Funct. Mater.*, 2020, **30**, 2004116; (*c*) J. Cao, H. Liu and H. Zhang, *CCS Chem.*, 2020, **2**, 2569–2575; (*d*) L. Lan, Q. Di, L. Li, B. Liu, X. Yu, P. Naumov and H. Zhang, *Cryst. Growth Des.*, 2022, **22**, 3435–3441.
10 For phase transitions of mechanically bent crystals with a shape-memory effect, see: (*a*) D. P. Karothu, J. Weston, I. T. Desta and P. Naumov, *J. Am. Chem. Soc.*, 2016, **138**, 13298–13306; (*b*) S. Takamizawa and Y. Takasaki, *Chem. Sci.*, 2016, **7**, 1527–1534; (*c*) C. Feng, T. Seki, S. Sakamoto, T. Sasaki, S. Takamizawa and H. Ito, *Chem. Sci.*, 2022, **13**, 9544–9551; (*d*) E. Ahmed, D. P. Karothu, M. Warren and P. Naumov, *Nat. Commun.*, 2019, **10**, 3723. For another example, see: (*e*) A. C. Maahs, M. G. Ignacio, M. Ghazzali, D. V. Soldatov and K. E. Preuss, *Cryst. Growth Des.*, 2017, **17**, 1390–1395.
11 Numerous studies regarding *e.g.*, polymorphism, emission properties, and mechanical bending of flufenamic acid have already been reported; for selected examples, see: (*a*) E. H. Lee, S. X. M. Boerrigter, A. C. F. Rumondor, S. P. Chamarthy and S. R. Byrn, *Cryst. Growth Des.*, 2008, **8**, 91–97; (*b*) V. López-Mejías, J. W. Kampf and A. J. Matzger, *J. Am. Chem. Soc.*, 2012, **134**, 9872–9875; (*c*) X. Wang, Y. Chen, J. Gong and J. Hou, *Org. Biomol. Chem.*, 2019, **17**, 3409–3415; (*d*) Y. Liu, P. Yang, K. Zhang, J. Xu, S. Wu and J. Gong, *Cryst. Growth Des.*, 2022, **22**, 1312–1318; (*e*) L. Waterloo, H. Hübner, F. Fierro, T. Pfeiffer, R. Brox, S. Löber, D. Weikert, M. Y. Niv and P. Gmeiner, *J. Med. Chem.*, 2023, **66**, 3499–3521.
12 Nanoindentation tests of **1α**, **1β**, and, **1γ** were performed (Fig. S4†).
13 T. Seki, K. Kobayashi, T. Mashimo and H. Ito, *Chem. Commun.*, 2018, **54**, 11136–11139.
14 The crystal structure of the bendable **1β** polymorph has similar characteristics to that of **1α**. The columns of **1β** are formed by the stacking of double hydrogen-bonded benzoic-acid moieties. Columns interact with neighboring columns *via* weak and strong intermolecular interactions (Fig. S7†).
15 (*a*) M. J. Turner, S. P. Thomas, M. W. Shi, D. Jayatilaka and M. A. Spackman, *Chem. Commun.*, 2015, **51**, 3735–3738; (*b*) K. B. Raju, S. Ranjan, V. S. Vishnu, M. Bhattacharya, B. Bhattacharya, A. K. Mukhopadhyay and C. M. Reddy, *Cryst. Growth Des.*, 2018, **18**, 3927–3937; (*c*) P. R. Spackman, M. J. Turner, J. J. McKinnon, S. K. Wolff, D. J. Grimwood, D. Jayatilaka and M. A. Spackman, *J. Appl. Crystallogr.*, 2021, **54**, 1006–1011; (*d*) M. Yoshida, Y. Makino, T. Sasaki, S. Sakamoto, S. Takamizawa, A. Kobayashi and M. Kato, *CrystEngComm*, 2021, **23**, 5891–5898.
16 The DFT calculations based on the single-crystal structures of **1α** and **1γ** indicate that the longer-wavelength emission of **1α** is most likely caused by the more pronounced intermolecular charge-transfer character of the excited state of **1α** compared to that of **1γ** (Fig. S13 and S14†).
17 NMR studies indicate that the crystalline lattice of $\mathbf{1}_{vapo}$ does not contain ethyl acetate (Fig. S16†).
18 The thermal phase transition of **1α** is rather complicated compared to the vapor-induced phase transition (Fig. S17 and S20†).
19 (*a*) L. Catalano, D. P. Karothu, S. Schramm, E. Ahmed, R. Rezgui, T. J. Barber, A. Famulari and P. Naumov, *Angew. Chem., Int. Ed.*, 2018, **57**, 17254–17258; (*b*) S. Hayashi, S. Yamamoto, D. Takeuchi, Y. Ie and K. Takagi, *Angew. Chem., Int. Ed.*, 2018, **57**, 17002–17008; (*c*) M. Nakabayashi, T. Matsuo and S. Hayashi, *Chem.–Eur. J.*, 2023, **29**, e202302351; (*d*) D. Tian and Y. Chen, *Adv. Opt. Mater.*, 2021, **9**, 2002264.